Supporting Informatiom

Hexagonal Nanoplates of High-quality γ-Gallium Oxide: Controlled Synthesis and Good Heterogeneous Catalytic Performance for Thiophenes**

Zun Yang, Le Xin Song,* Ya Qian Wang, Mao Mao Ruan, Yue Teng, Juan Xia, Jun Yang, Shan Shan Chen and Fang Wang

*University of Science and Technology of China, Hefei 230026, China
E-mail: solexin@ustc.edu.cn;

A list of the contents for all the Supporting Information

Supporting Informatiom

Experimental Section

Preparation of the Ga_2O_3 materials: In the preparation experiments, all the reagents were analytical grade and were used without further purification. The γ-Ga_2O_3-np was synthesized by a facile hydrothermal process: Initially, metal gallium (0.05 g, 0.7 mmol) was dissolved in HCl (30 mL, 0.4 M) to form an aqueous solution of Ga^{3+} ions. Then, 0.50 g of urea (8.3 mmol) and 0.39 g of POM (2.1 mmol, the mole ratio of $GaCl_3$ to POM, 1:3) and 78 mg of PVP (k-30, 0.7 mmol PVP units) were added to the solution under vigorous stirring for 0.5 h at room temperature. Subsequently, this solution was transferred into a Teflon-lined stainless steel autoclave (50 mL). The autoclave was maintained at 453 K for 3 h, and then cooled gradually to ambient temperature. Finally, a white product (γ-Ga_2O_3-np, 65 mg, 99%) was obtained by filtration and washing several times with distilled water and absolute ethyl alcohol, then dried at vacuum at 373 K for 10 h. The γ-Ga_2O_3-mf was prepared by the same method as the γ-Ga_2O_3-np when PVP was absent. All other samples were synthesized using a similar procedure by varying reaction parameters, including concentration, temperature, and reaction time. The β-Ga_2O_3-np and β-Ga_2O_3-mf was obtained by sintering the γ-Ga_2O_3-np and γ-Ga_2O_3-mf at 1073 K for 3 h in air, respectively.

Preparation of the PVP-Ga^{3+} and PVP-TOG: 20 mL aqueous solution containing 0.5 mmol PVP units (55.5 mg) and 0.5 mmol $GaCl_3$ (88.3 mg, the molar ratio of $GaCl_3$ to PVP, 1:1) was stirred for 3 h at 333 K in a round-bottom flask using oil bath heating; then, water was removed from the solution by rotary evaporation below 323 K. Finally, the PVP-Ga^{3+} was obtained after drying to constant weight at 373 K for 10 h. The PVP-TOG was gained by the similar way by mixing 0.5 mmol PVP, 0.5 mmol $GaCl_3$ and 1.5 mmol POM (276 mg), and stirring for 9 h at 333 K.

Catalytic experiments: A 10.0 mL solution of TP (1.60×10^{-4} mol·dm^{-3} in *n*-octane) was placed in a three neck round bottom flask fitted with a thermometer, a reflux condenser and an inlet for the addition of a 10.0 mL solution of H_2O_2 (9.70×10^{-3} mol·dm^{-3} in water). Initially, the mixed solutions of TP and H_2O_2 were heated to 343 K. Subsequently, Ga_2O_3 (0.08 mmol, 15 mg) was added to the mixed solutions. Then, the solutions were vigorously stirred for 2 h at this temperature. Finally, the organic phase was separated from the aqueous phase by centrifugation and analyzed using UV-Vis spectrophotometer to determine the content of TP in the organic phase. The oxidative desulfurization of TP derivatives were conducted in the similar conditions as the TP. The catalyst was recycled by washing several times with absolute ethyl alcohol, separating and drying at vacuum at 373 K for 10 h.

Material characterization: X-ray diffraction (XRD) measurements were performed on a Philips X'Pert Pro X-ray diffractometer using a monochromatized Cu Kα radiation source (40 kV, 40 mA) with a wavelength of 0.1542 nm and analyzed in the range $10° \leq 2\theta \leq 80°$. Field emission scanning electron microscope (FE-SEM) images were recorded by using a Supra 40 operated at 5 kV. The typical high resolution transmission electron microscopy (HR-TEM) images and selected area electron diffraction (SAED) patterns were taken on a JEF 2100F field-emission transmission electron microscope performing at 200 kV. Thermogravimetry (TG) was performed on a DTGA-60H thermogravimetric analyzer under a nitrogen atmosphere with a gas flow of 25 mL·min^{-1}. Fourier transform infrared (FT-IR) spectra were obtained on a Bruker Equinox 55 spectrometer with KBr pellets in the range of 400~4000 cm^{-1} with a resolution of less than 0.09 cm^{-1}. Raman spectra were recorded with a Renishaw InVia Raman Microscope at room temperature with 532 nm laser excitation in the range 100-1800 m^{-1}, with a resolution of 0.6 cm^{-1}. Nitrogen adsorption/desorption isotherms were obtained using Micromeritics ASAP-2000 Surface Area and Porosimetry System at 77 K. The ^{1}H and ^{13}C nuclear magnetic resonance (NMR) spectra were recorded on a Bruker Avance 300 NMR spectrometer at 300 MHz at ambient temperature unless otherwise stated. UV-Vis spectra were done with a Shimadzu UV 3600 spectrometer in the range of 200~600 nm. X-ray photoelectron spectroscopy (XPS) measurements were done using an ESCALAB 250 spectrometer with Al Kα radiation (1486.6 eV) in ultra-high vacuum (2.00×10^{-9} Torr). And all of the values of binding energy were referenced to C1s peak (284.8 eV) with an energy resolution of 0.16 eV. High-performance liquid chromatography (HPLC) analysis was performed on Aglient Technologies 1260 (250×4.6 mm, 5 μm; 303 K; methanol/water [80/20, *v*/*v*]; flow rate: 1.0 mL·min^{-1}). The conductivity experiments were conducted in a Leici DDSJ-308 conductivity meter (Shanghai Leici Instrument factory) with automatic temperature compensation at 298 K and automatic calibration.

Supporting Informatiom

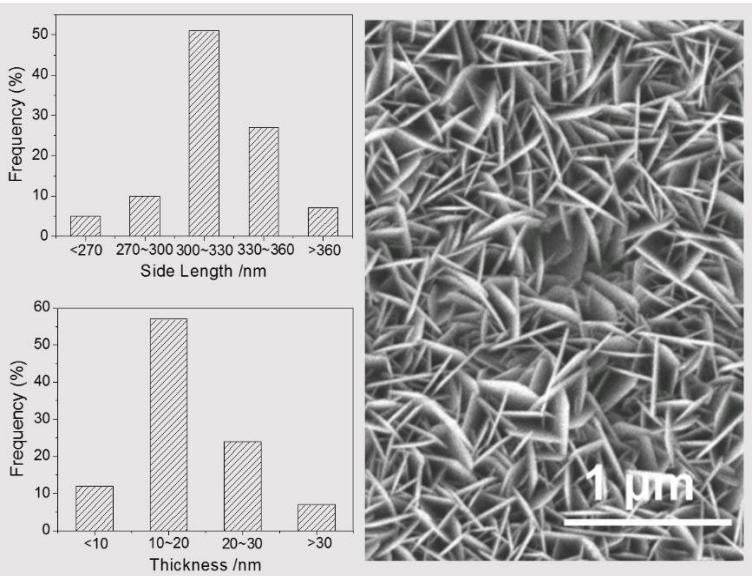

Figure S1. The size distribution of the γ-Ga_2O_3-np.

Supporting Informatiom

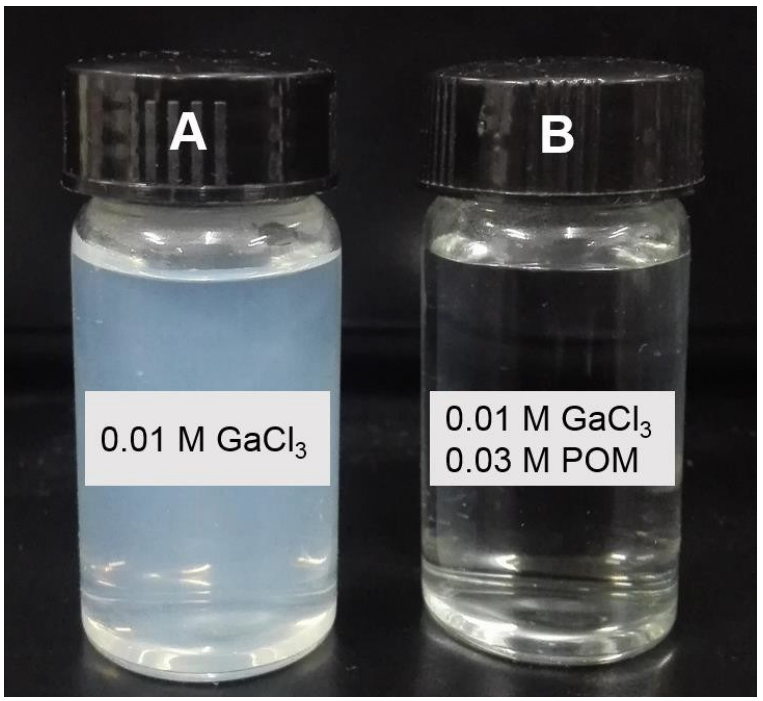

Figure S2. The addition of small amounts of POM into a $GaCl_3$ solution (stirring for 2 h at 333 K) leads to a quick change from turbid to transparent.

Supporting Informatiom

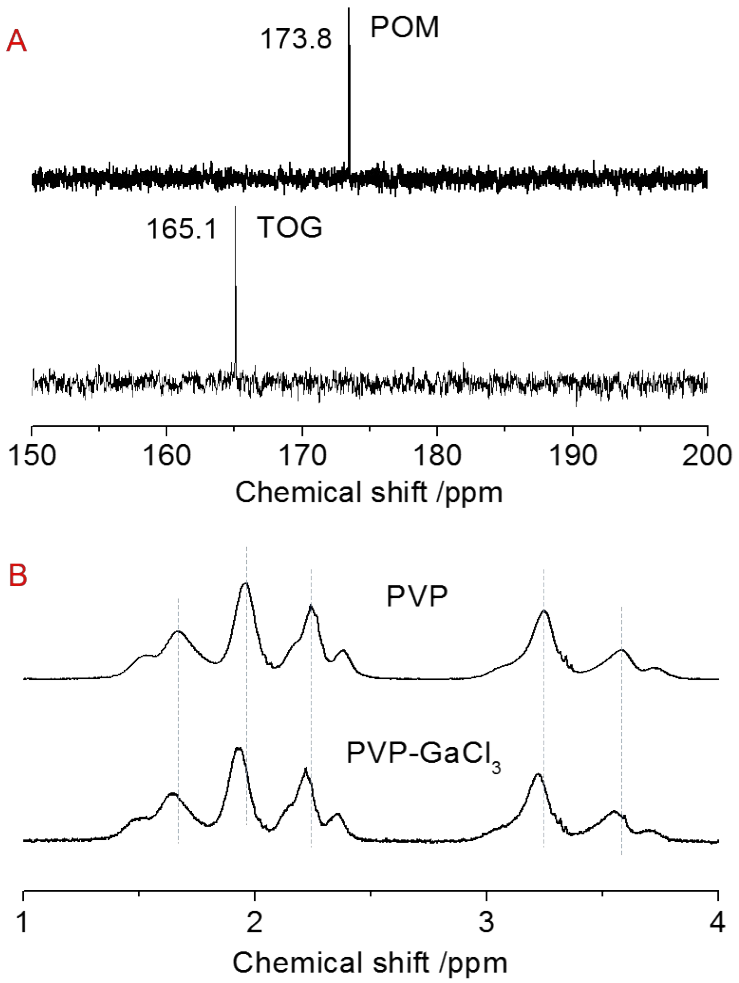

Figure S3. A) The ^{13}C NMR spectra of POM and its complex of Ga^{3+} (TOG); B) The ^{1}H NMR spectra of PVP and the PVP-$GaCl_3$: ^{1}H NMR (300 MHz, D_2O, 298 K, ppm) of free PVP: δ 3.669 (C*H*N), 3.248 (CH_2N), 2.316 (CH_2CO), 1.966 (CH_2CCO), 1.594 (CH_2CH). ^{1}H NMR (300 MHz, D_2O, 298 K, ppm) of PVP-$GaCl_3$: δ 3.620 (C*H*N), 3.222 (CH_2N), 2.293 (CH_2CO), 1.935 (CH_2CCO), 1.561 (CH_2CH).

Supporting Informatiom

The coordination interaction between Ga^{3+} and Ox^{2-} ions was confirmed by Raman analysis. The Raman curve of the TOG complex shows a characteristic peak at 573 cm^{-1} due to the Ga-O stretching vibration mode of Ga(III)-COO^{-} complex,[1] which is different from the GaO vibration mode of γ-Ga_2O_3.[2] The peaks with wavenumbers lower than 400 cm^{-1} are due to the deformation vibration modes of CCO, OGaO and COGa.[1]

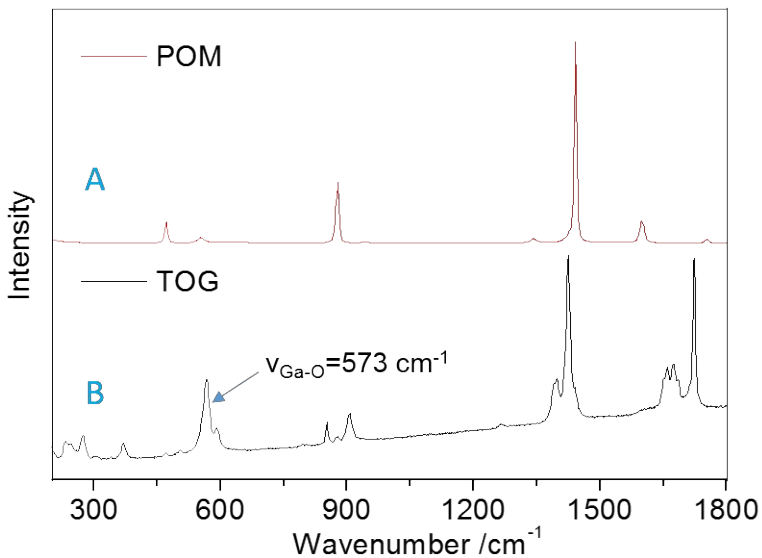

Figure S4. The Raman spectra of the POM (A) and TOG (B).

References

[1] D R. E. Hester, R. A. Plane, *Inorg. Chem.* **1964**, *3*, 513.

[2] H. Seshadri, M. Cheralathan, P. Sinha, *Res. Chem. Intermediat.* **2013**, *39*, 991.

Supporting Informatiom

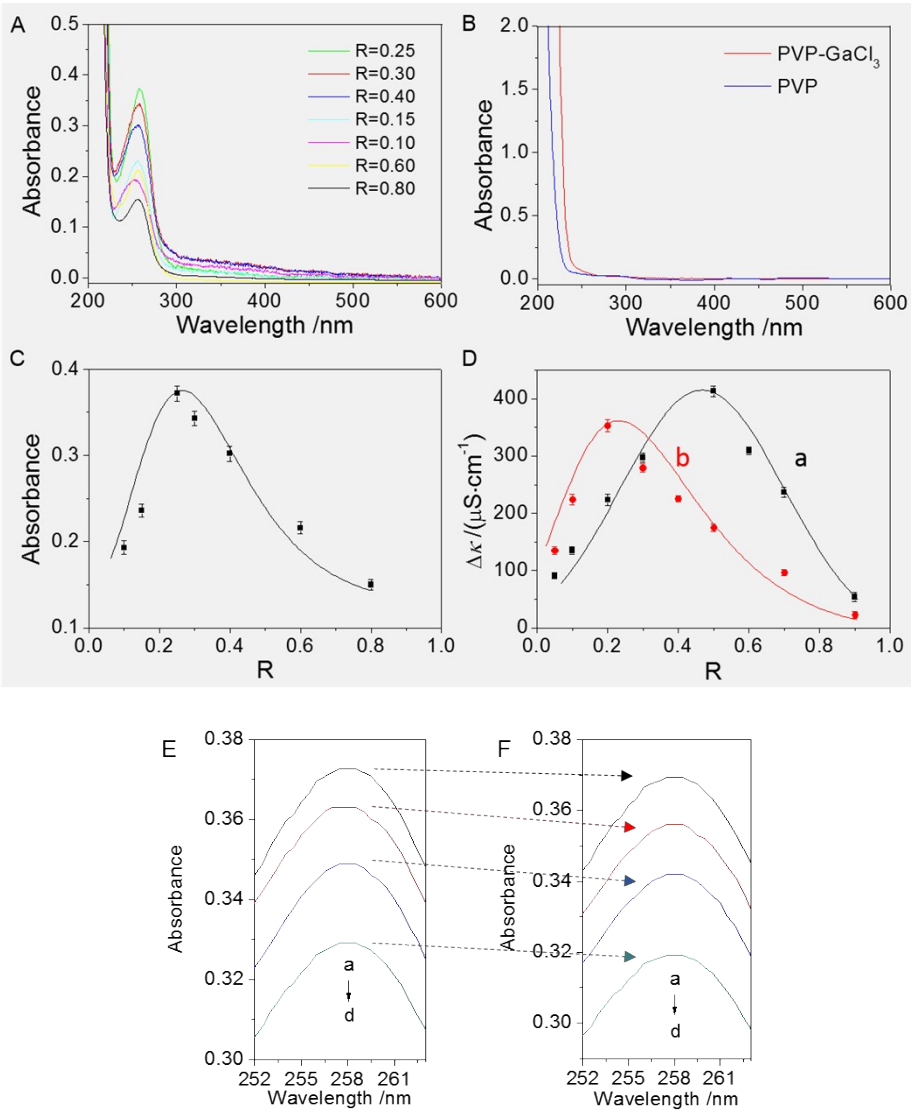

Figure S5. (A, C) The UV-Vis spectra and Job's plot of the solutions (total moles, TM) of $GaCl_3$ and POM (the R is a molar ratio of $GaCl_3$ to the TM). (B) The UV-Vis spectra of PVP (2.50×10^{-3} M) and PVP-$GaCl_3$ (2.50×10^{-3} M). (D) The Job's plots ($\Delta\kappa$ represents the decrease in electric conductivity) of the solutions of $GaCl_3$ and its complex upon addition of PVP: a) PVP and $GaCl_3$ (total moles, TM, the R is a molar ratio of $GaCl_3$ to the TM); b) PVP and TOG (total moles, TM, the R is a molar ratio of TOG to the TM). (E, F) An estimation of the formation rate of the complex based on its concentration reflected by the absorption peak of the Ga-O coordination bonds at 257.6 nm. The UV-Vis spectra of the solutions of $GaCl_3$ (2.50×10^{-3} M) with POM (7.50×10^{-3} M) in the absence (E) and presence (F) of PVP (78 mg) at different reaction times: a) 120, b) 90, c) 60, d) 30 min. Clearly, the introduction of PVP results in a decrease of the formation rate of the Ga-O coordination bonds.

Supporting Informatiom

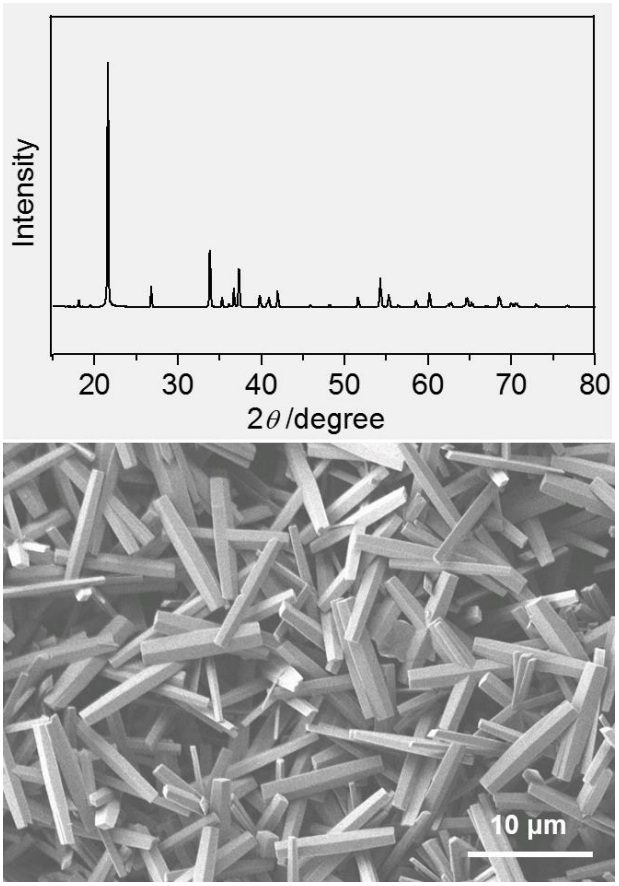

Figure S6. The XRD pattern and FE-SEM image of the GaOOH sample obtained when POM was completely substituted by PVP.

Supporting Informatiom

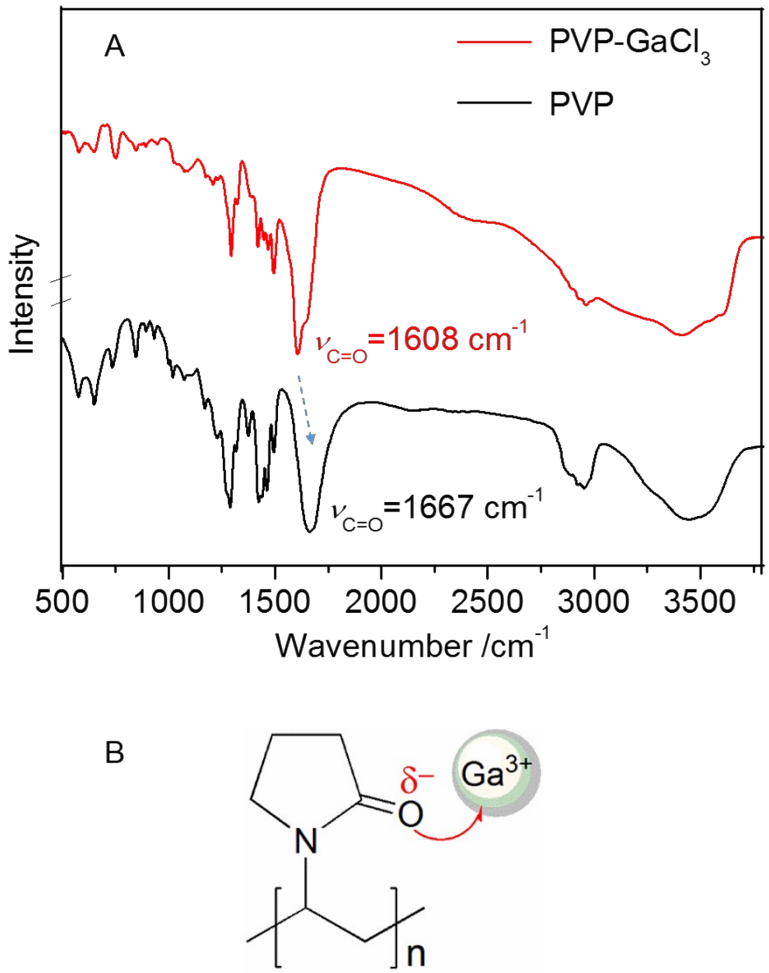

Figure S7. (A) The FT-IR spectra of PVP and the PVP-$GaCl_3$; (B) The ion-dipole interaction between PVP and Ga^{3+}.

Supporting Informatiom

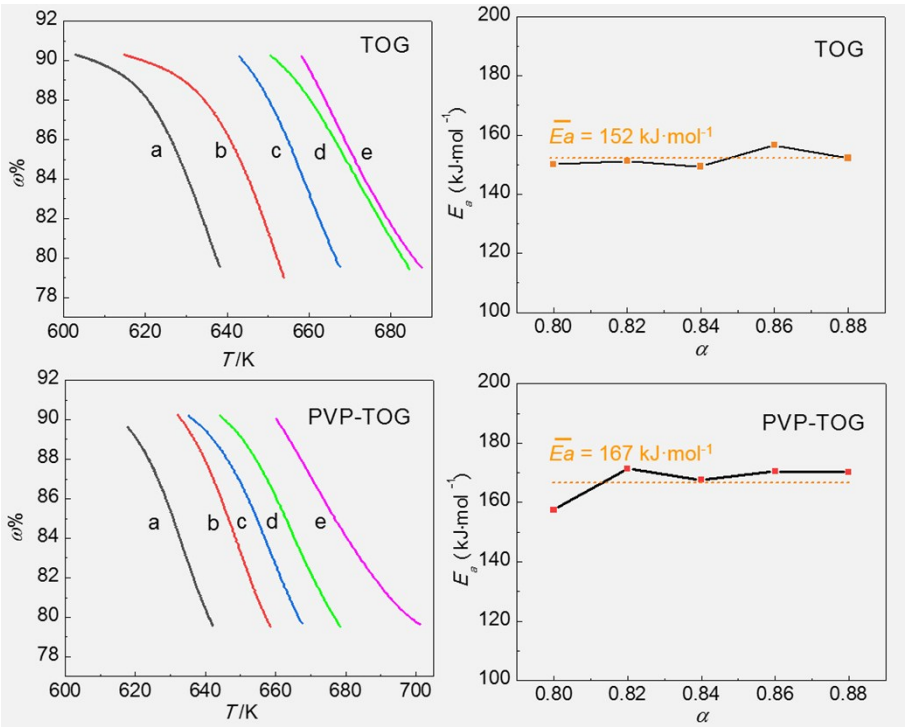

Figure S8. TG profiles and E_a values of TOG and PVP-TOG, a~e represent different heating rates: a) 5, b) 10, c) 15, d) 20, e) 25 K·min^{-1}, α represents the residual mass fraction (%).

Supporting Informatiom

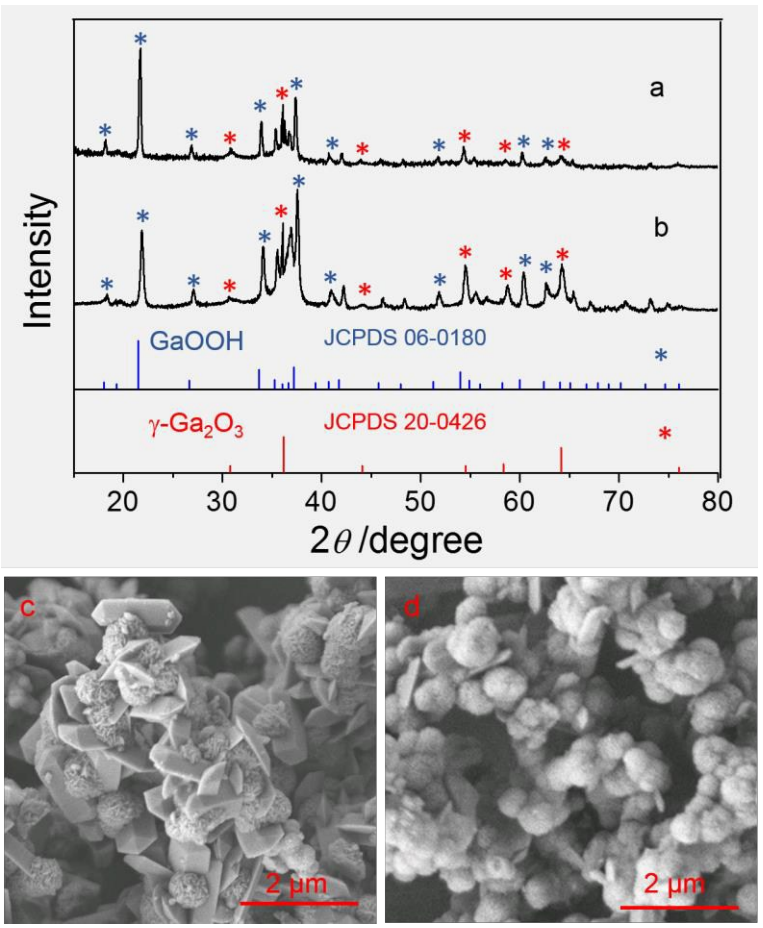

Figure S9. The XRD patterns and FE-SEM images of the products (a mixture of GaOOH and γ-Ga_2O_3) obtained using the same conditions as Figure 1b when urea was substituted by NaOH (a, c) and ammonia (b, d) to adjust the pH.

Supporting Informatiom

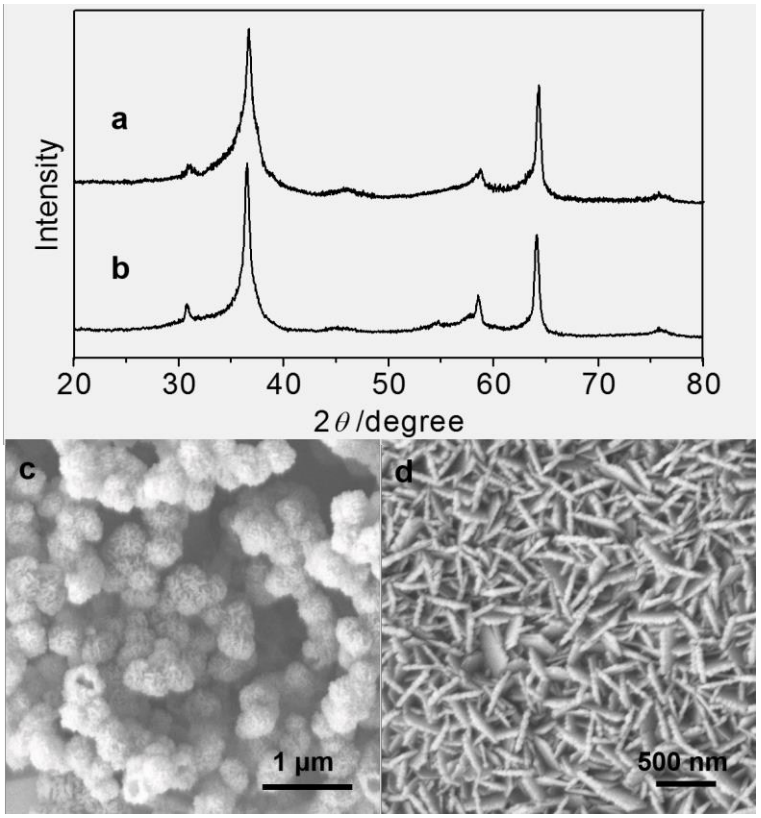

Figure S10. The XRD patterns and FE-SEM images of the γ-Ga_2O_3 samples obtained using the same conditions as Figure 1b at different temperatures: 433 K (a, c) and 473 K (b, d).

Supporting Informatiom

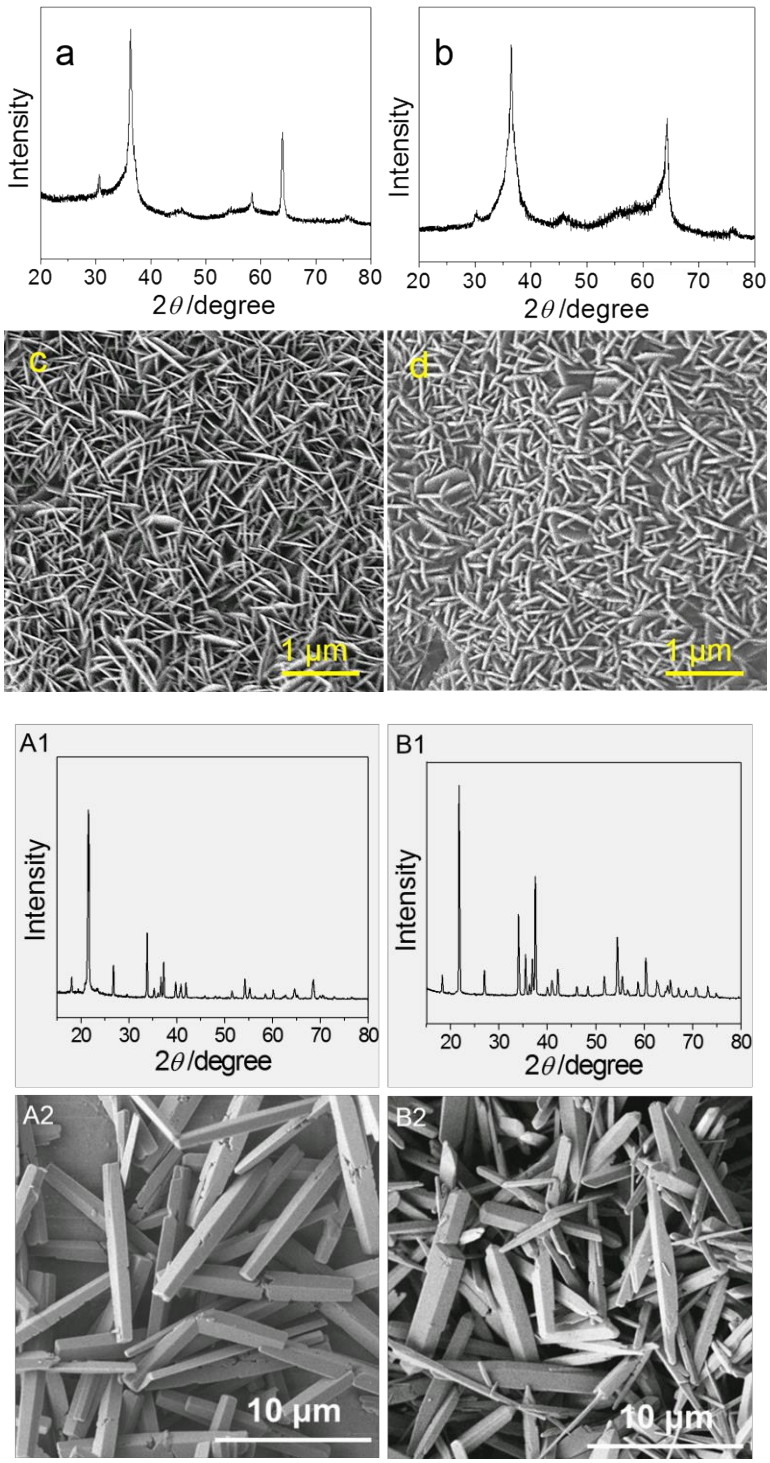

Figure S11. The XRD patterns and FE-SEM images of the samples obtained using the same conditions as Figure 1b but with different ligands: OAD (a, c), MA (b, d), EDA (A1, A2) and EG (B1, B2).

Supporting Informatiom

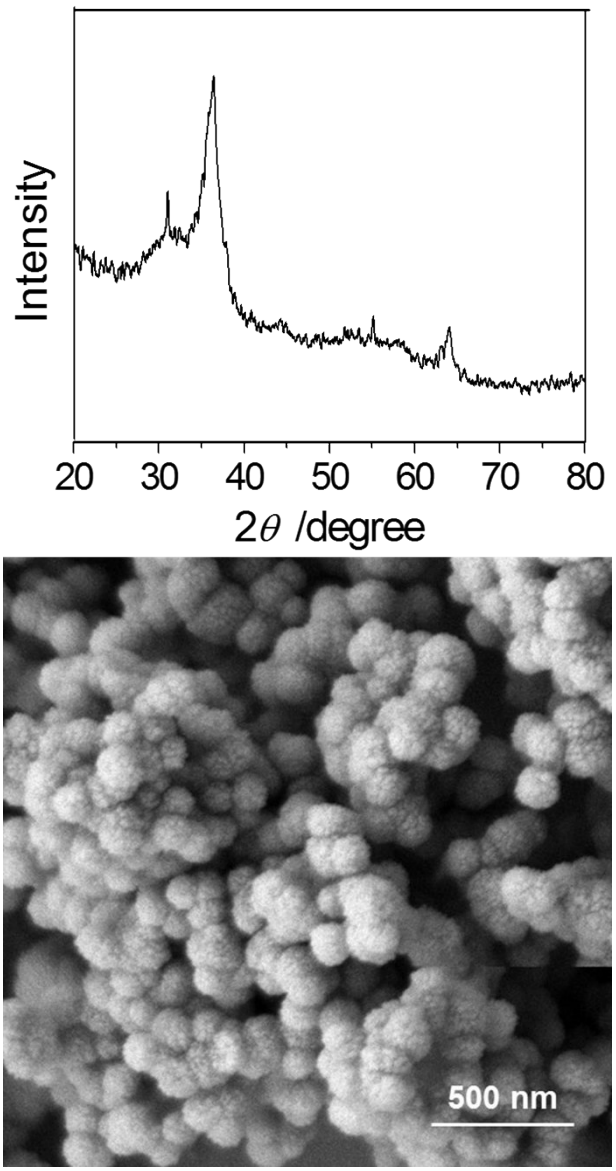

Figure S12. The XRD pattern and FE-SEM image of the γ-Ga_2O_3 sample obtained using the same conditions as Figure 1b when POM was substituted by CA with a reaction time of 6 h.

Supporting Informatiom

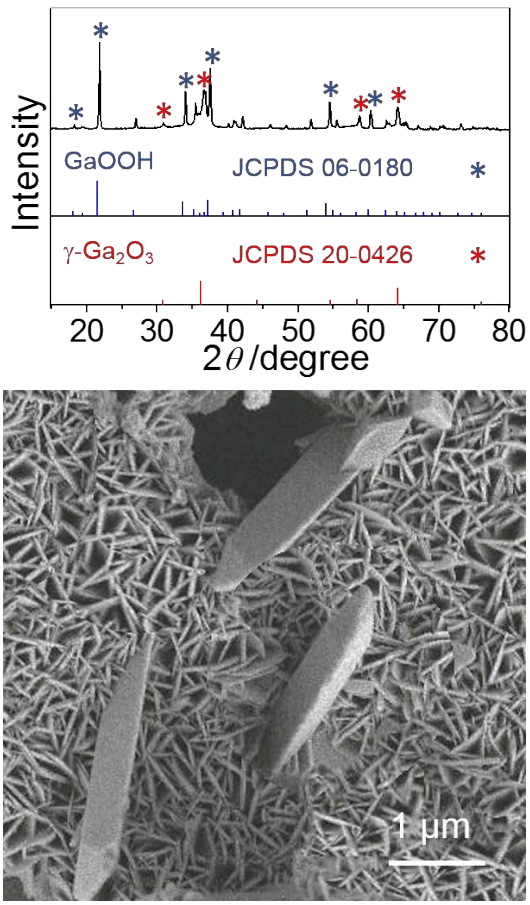

Figure S13. The XRD pattern and FE-SEM images of the sample obtained using the same conditions as Figure 1b when the molar ratio of POM to $GaCl_3$ is 1.5:1.

Supporting Informatiom

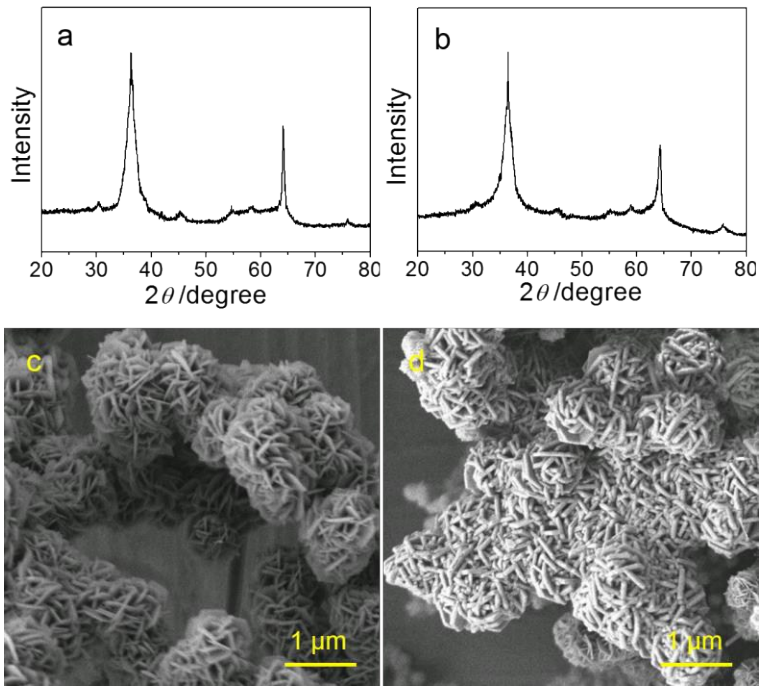

Figure S14. The XRD patterns and FE-SEM images of the sample obtained using the same conditions as Figure 1b when the PVP was substituted by PVC (a, c) and β-CD (b, d).

Supporting Informatiom

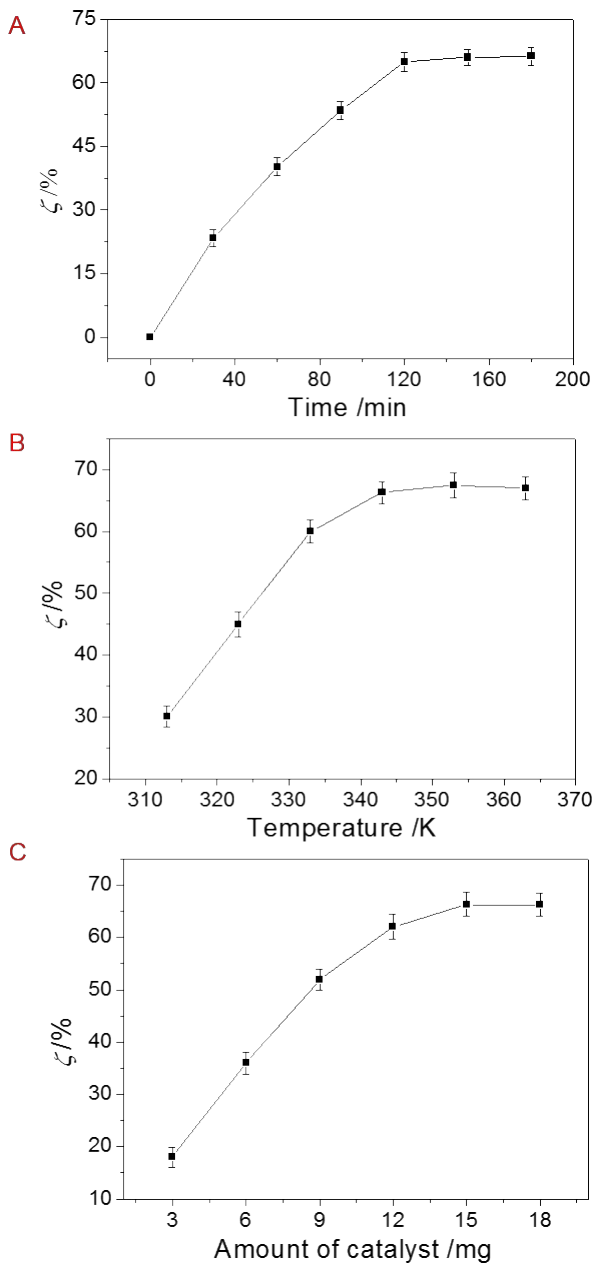

Figure S15. Thiophene conversions of the γ-Ga_2O_3-np with H_2O_2 in *n*-octane: (A) at 343 K using the catalyst amount of 15 mg with different times (0, 30, 60, 90, 120, 150, 180 min); (B) at different temperatures (313, 323, 333, 343, 353 and 363 K) using the catalyst amount of 15 mg for 2 h, and (C) at 343 K using different catalyst amounts (3, 6, 9, 12, 15 and 18 mg) for 2 h.

Supporting Informatiom

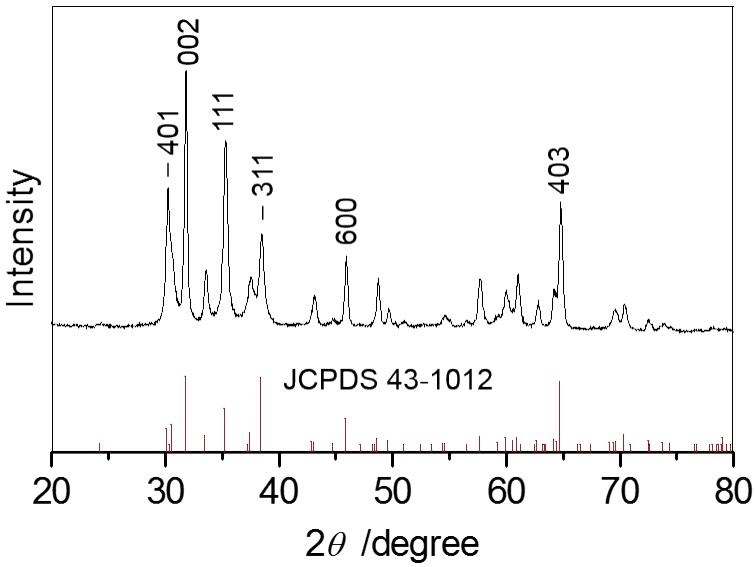

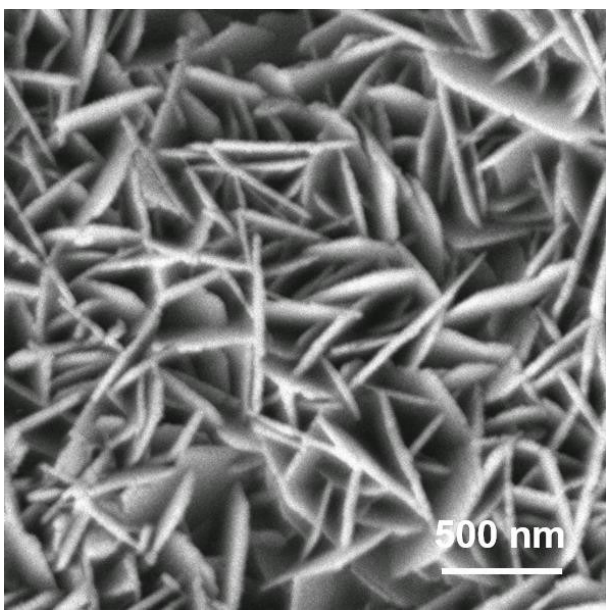

Figure S16. The XRD pattern and FE-SEM image of the β-Ga_2O_3-np sample obtained by sintering the γ-Ga_2O_3-np at 1073 K for 3 h in air.

Supporting Informatiom

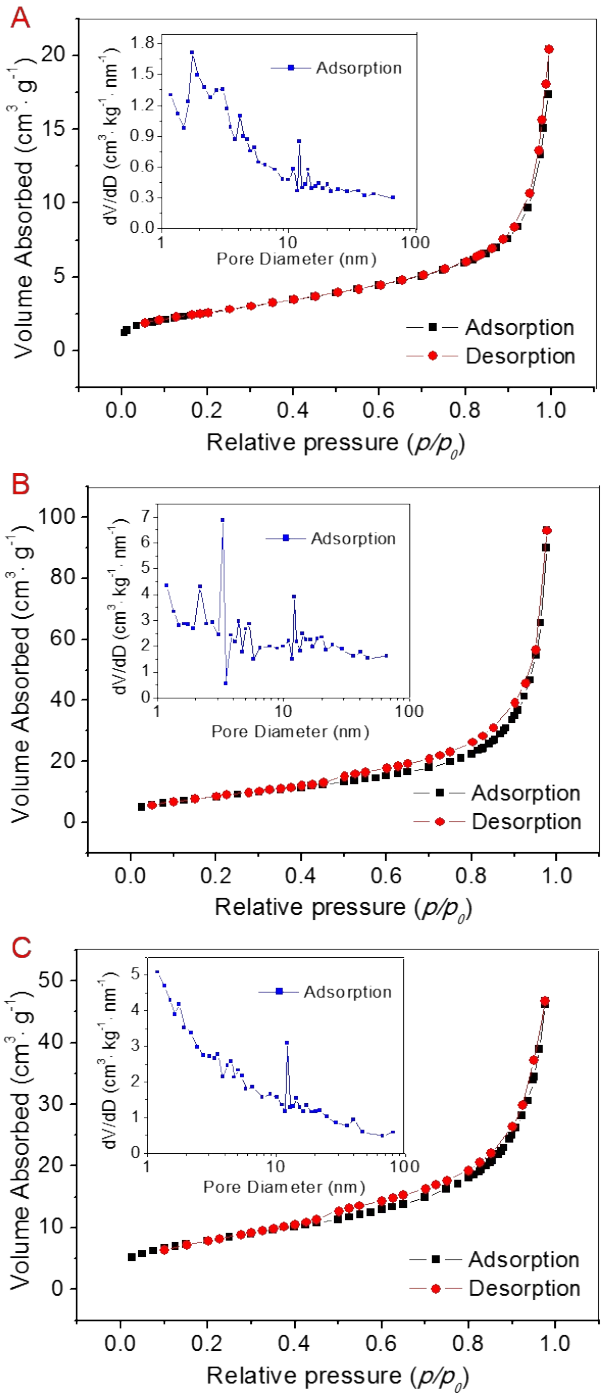

Figure S17. The N_2 adsorption-desorption isotherms and pore size distributions (see the insets) of the β-Ga_2O_3-np (A), γ-Ga_2O_3-np (B) and γ-Ga_2O_3-mf (C) .

5

Supporting Informatiom

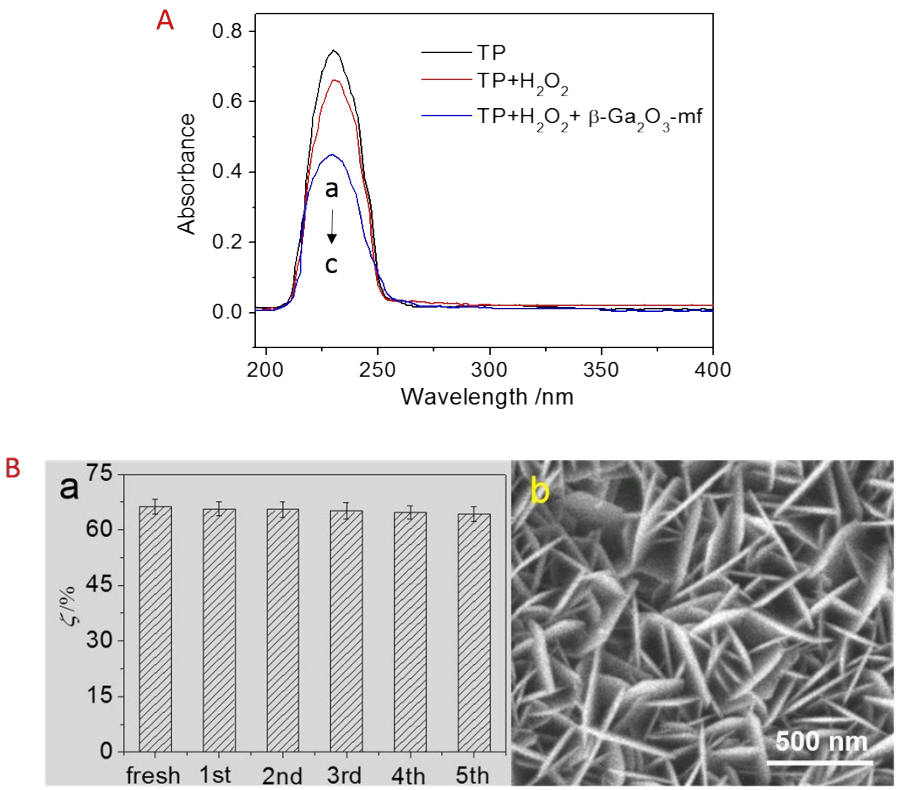

Figure S18. (A) UV-Vis spectra of TP in organic phase under different systems in *n*-octane: (a) TP, (b) TP + H_2O_2, (c) TP + H_2O_2 + β-Ga_2O_3-mf; (B) (a) the bar diagram depicting the ζ values of the γ-Ga_2O_3-np in the first five runs, and (b) FE-SEM image of the used γ-Ga_2O_3-np after the 5th run.

Supporting Informatiom

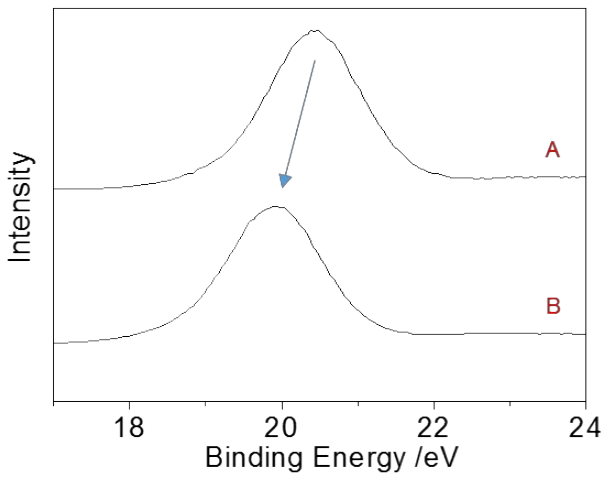

Figure S19. Ga 3d XPS spectra of the γ-Ga_2O_3-np samples impregnated with H_2O (A) and aqueous H_2O_2 (B, 9.70×10^{-3} mol·dm^{-3}).

Supporting Informatiom

Figure S20 shows that there is only a peak at 2.99 min of retention time. It is ascribed to either TP-oxide or TP-dioxide because the peak of free TP occurred at 5.76 min of retention time. The FT-IR analysis displays that there are two strong bands at 1155 cm^{-1} and 1247 cm^{-1}, which can be attributed to the symmetric and asymmetric vibration modes of S-O in the TP-dioxide, respectively.[1~3]

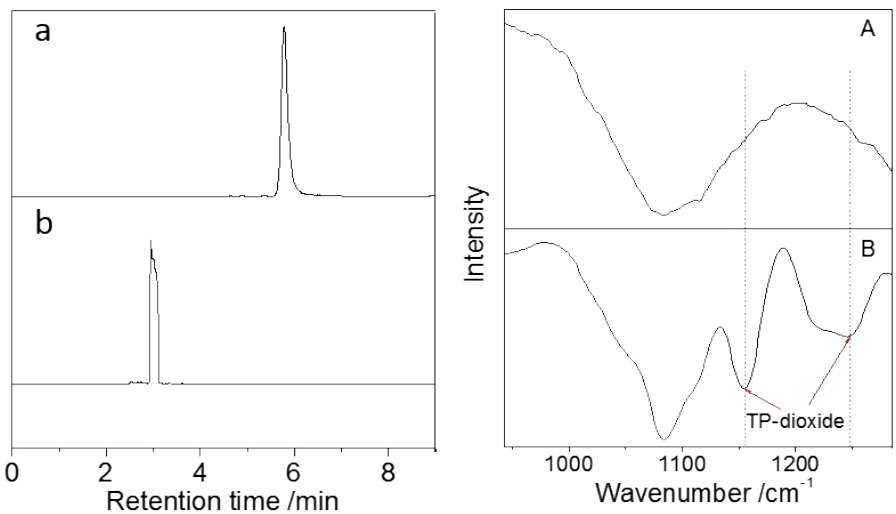

Figure S20. HPLC analysis of TP (a) and TP-dioxide (b), and FT-IR spectra of the γ-Ga_2O_3-np before (A) and after (B) the catalytic oxidation of TP. The strong absorption peak in 1050~1100 cm^{-1} are due to a characteristic vibration band of γ-Ga_2O_3.[4]

References

[1] J. Nakayama, H. Nagasawa, Y. Sugihara, A. Ishii, *J. Am. Chem. Soc.* **1997**, *119*, 9077.
[2] A. Nisar, Y. Lu, J. Zhuang, X. Wang, *Angew. Chem. Int. Edit.* **2011**, *123*, 3245.
[3] S. Otsuki, T. Nonaka, N. Takashima, W. Qian, A. Ishihara, T. Imai, T. Kabe, *Energy Fuels* **2000**, *14*, 1232.
[4] H. Seshadri, M. Cheralathan, P. K. Sinha, *Res. Chem. Intermediat.* **2012**, *39*, 991.

Supporting Informatiom

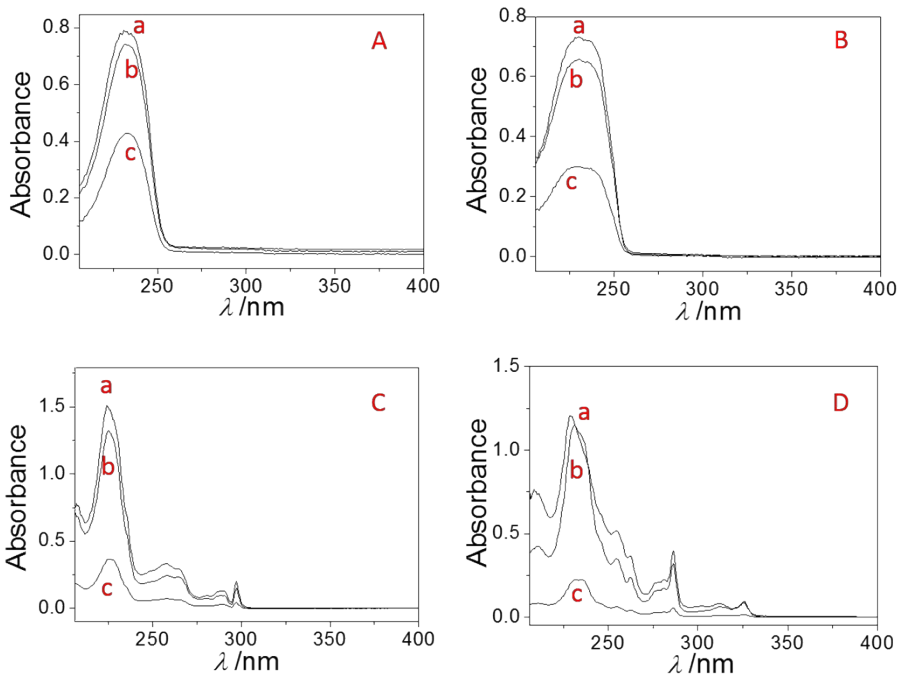

Figure S21. UV-Vis spectra of residual 2-MTP (A), 3-MTP (B), BTP (C) and DBTP (D) in organic phase under different systems in *n*-octane (a); with H_2O_2 in *n*-octane (b); and with H_2O_2 and γ-Ga_2O_3-np in *n*-octane (c).

Supporting Informatiom

Table S1. The ζ values of different catalysts in the oxidative desulfurization.

Catalysts	*t* /min	*T* /K	M[a] g/L	Solvents	ζ /%					Ref
					TP	2-MTP	3-MTP	BTP	DBTP	
γ-Ga_2O_3	120	343	0.75	water	66.3	45.5	58.7	76.2	80.6	This work
MoO_3	240	353	0.6	water	30	–	–	–	–	1
AMT[b]	120	353	0.16	water	33	45	13	–	–	2
Mo/Al_2O_3	60	333	1.36	AC[f]	0.2	–	–	64.2	98.7	3
MoO_3/Al_2O_3	60	333	3.3	AC	–	–	–	–	70.5	4
Sn/Al_2O_3	30	333	–	DMF	62	–	–	–	60	5
Fe/Al_2O_3	30	333	–	DMF	57	–	–	–	55	5
Ti-beta[c]	300	343	3.2	water	–	–	–	64.3	25	6
Mo-LDH[d]	180	313	–	AC	–	–	–	45	60.5	7
CeO_2	30	303	3.3	$[C_8mim]BF_4$[g]	–	–	–	–	38.5	8
ZrO_2	120	333	2	AC	–	–	–	–	17	9
V_2O_5	120	333	2	AC	–	–	–	–	37	9
WOx/ZrO_2	180	348	1.3	AC	65	–	–	91	–	10
V-HMS[e]	60	333	–	AC	–	–	–	18	62	11
Mn_3O_4	20	333	–	AC	65	–	–	57	46	12
TiO_2	60	333	0.5	AC	–	–	–	–	39	13
VOx/TiO_2	90	333	2	AC	–	–	–	–	67.9	14
CeO_2/TiO_2	300	–	1	water	–	–	–	90	–	15
CeO_2	300	–	1	water	–	–	–	< 40	–	15
TiO_2	300	–	1	water	–	–	–	< 45	–	15
Ni-CuO/$BiVO_4$	180	283	1	AC	94	–	–	–	–	16
Ni/$BiVO_4$	180	283	1	AC	43	–	–	–	–	16
CuO/$BiVO_4$	180	283	1	AC	42	–	–	–	–	16
$BiVO_4$	180	283	1	AC	40	–	–	–	–	16

[a] Amount of catalysts; [b] Ammonium molybdate tetrahydrate; [c] Ti-containing molecular sieve; [d] Mo-containing layered double hydroxide; [e] V-containing hexagonal mesoporous silica; [f] Acetonitrile; [g] 1-*n*-octyl-3-methylimidazolium tetrafluoroborate.

References

[1] L. X. Song, M. Wang, S. Z. Pan, J. Yang, J. Chen, J. Yang, *J. Mater. Chem.* **2011**, *21*, 7982.

[2] L. X. Song, M. Wang, Z. Dang, F. Y. Du, *J. Phys. Chem. B* **2010**, *114*, 3404.

[3] J. L. García-Gutiérrez, G. A. Fuentes, M. E. Hernández-Terán, F. Murrieta, J. Navarrete, F. Jiménez-Cruz, *Appl. Catal. A* **2006**, *305*, 15.

[4] J. L. García-Gutiérrez, G. A. Fuentes, M. E. Hernández-Terán, P. Garcia, F. Murrieta-Guevara, F. Jiménez-Cruz, *Appl. Catal. A* **2008**, *334*, 366.

[5] W. A. W. A. Bakar, R. Ali, A. A. A. Kadir, W. N. A. W. Mokhtar, *Fuel Process. Technol.* **2012**, *101*, 78.

Supporting Informatiom

[6] V. Hulea, F. Fajula, J. Bousquet, *J. Catal.* **2001**, *198*, 179.
[7] A.-L. Maciuca, C.-E. Ciocan, E. Dumitriu, F. Fajula, V. Hulea, *Catal. Today* **2008**, *138*, 33.
[8] M. Zhang, W. Zhu, S. Xun, H. Li, Q. Gu, Z. Zhao, Q. Wang, *Chem. Eng. J.* **2013**, *220*, 328.
[9] L. Fabián-Mijangos, L. Cedeño-Caero, *Ind. Eng. Chem. Res.* **2010**, *50*, 2659.
[10] Z. Hasan, J. Jeon, S. H. Jhung, *J. Hazard. Mater.* **2012**, *205*, 216.
[11] Y. Shiraishi, T. Naito, T. Hirai, *Ind. Eng. Chem. Res.* **2003**, *42*, 6034.
[12] B. Zapata, F. Pedraza, M. A. Valenzuela, *Catal. Today* **2005**, *106*, 219.
[13] U. Arellano, J. Wang, M. Timko, L. Chen, S. P. Carrera, M. Asomoza, O. G. Vargas, M. Llanos, *Fuel* **2014**, *126*, 16.
[14] M. A. Ramos-Luna, L. Cedeño-Caero, *Ind. Eng. Chem. Res.* **2010**, *50*, 2641.
[15] X. Lu, X. Li, J. Qian, N. Miao, C. Yao, Z. Chen, *J. Alloy. Compd.* **2016**, *661*, 363.
[16] F. Lin, Z. Shao, P. Li, Z. Chen, X. Liu, M. Li, B. Zhang, J. Huang, G. Zhu, B. Dong, *RSC Adv.* **2017**, *7*, 15053.